

1  
2  
3 **Enzymatic crosslinking of dynamic thiol-norbornene click hydrogels**  
4

5 Han D. Nguyen, Hung-Yi Liu, Britney N. Hudson, and Chien-Chi Lin\*  
6

7  
8 *Department of Biomedical Engineering, Purdue School of Engineering & Technology,*  
9

10 *Indiana University-Purdue University Indianapolis, Indianapolis, IN 46202, USA*  
11  
12  
13  
14  
15  
16  
17  
18  
19  
20  
21  
22  
23  
24  
25

26  
27 \*To whom correspondence should be sent:  
28  
29  
30

31 Chien-Chi Lin, PhD.  
32 Associate Professor  
33 Department of Biomedical Engineering  
34 Purdue School of Engineering & Technology  
35 Indiana University-Purdue University Indianapolis  
36 Indianapolis, IN 46202  
37 Phone: (317) 274-0760  
38 Email: [lincc@iupui.edu](mailto:lincc@iupui.edu)  
39  
40  
41  
42  
43  
44  
45  
46  
47  
48  
49  
50  
51  
52  
53  
54  
55

---

This is the author's manuscript of the article published in final edited form as:

Nguyen, H. D., Liu, H.-Y., Hudson, B. N., & Lin, C.-C. (2019). Enzymatic crosslinking of dynamic thiol-norbornene click hydrogels. ACS Biomaterials Science & Engineering. <https://doi.org/10.1021/acsbiomaterials.8b01607>

## Abstract

Enzyme-mediated *in situ* forming hydrogels are attractive for many biomedical applications because gelation afforded by the enzymatic reactions can be readily controlled not only by tuning macromer compositions, but also by adjusting enzyme kinetics. For example, horseradish peroxidase (HRP) has been used extensively for *in situ* crosslinking of macromers containing hydroxyl-phenol groups. The use of HRP on initiating thiol-allylether polymerization has also been reported, yet no prior study has demonstrated enzymatic initiation of thiol-norbornene gelation. In this study, we discovered that HRP can generate thiyl radicals needed for initiating thiol-norbornene hydrogelation, which has only been demonstrated previously using photopolymerization. Enzymatic thiol-norbornene gelation not only overcomes light attenuation issue commonly observed in photopolymerized hydrogels, but also preserves modularity of the crosslinking. In particular, we prepared modular hydrogels from two sets of norbornene-modified macromers, 8-arm poly(ethylene glycol)-norbornene (PEG8NB) and gelatin-norbornene (GeINB). Bis-cysteine-containing peptides or PEG-tetra-thiol (PEG4SH) were used as crosslinkers for forming enzymatically and orthogonally polymerized hydrogels. For HRP-initiated PEG-peptide hydrogel crosslinking, gelation efficiency was significantly improved via adding tyrosine residues on the peptide crosslinkers. Interestingly, these additional tyrosine residues did not form permanent dityrosine crosslinks following HRP-induced gelation. As a result, they remained available for tyrosinase-mediated secondary crosslinking, which dynamically increases hydrogel stiffness. In addition to material characterizations, we also found that both PEG- and gelatin-based hydrogels provide excellent cytocompatibility for dynamic 3D cell culture. The enzymatic thiol-norbornene gelation scheme presented here offers a new crosslinking mechanism for preparing modularly and dynamically crosslinked hydrogels.

**Keywords:** Dynamic hydrogels, Horseradish peroxidase, Glucose oxidase, Thiol-norbornene click chemistry.

## 1. Introduction

Hydrogels prepared from orthogonal crosslinking methods have tremendous potential in drug delivery and tissue engineering applications.[1-3] In particular, thiol-norbornene click reaction is advantageous in hydrogel crosslinking owing to the rapid and quantitative reactivity between thiol- and norbornene-functionalized macromers.[4-9] The modular and orthogonal reactivity of thiol-norbornene click reaction has been used to fabricate a diverse array of biomaterials, including bulk hydrogel,[10-12] colloidal gel,[13, 14] as well as cell surface coating.[15] Current modular thiol-norbornene hydrogels are exclusively prepared from photopolymerizations initiated by ultraviolet (UV) light, visible light, or two photon irradiation.[4, 5, 9, 16-20] While photopolymerization affords spatial-temporal control in crosslinking, hydrogels formed by photochemistry are typically limited in thickness/depth due to light attenuation in thick/dark samples. For clinical applications, UV light absorption by the skin also reduces the utility of photopolymerized hydrogels.[21] It will be ideal if the synthetically simple thiol-norbornene hydrogels could be prepared with high injectability and any given sizes and shapes without sacrificing modularity of the crosslinking.

The light attenuation issue of photopolymerization can be overcome by exploiting enzymatic reaction capable of generating thiyl radicals needed for the initiation of thiol-norbornene reaction.[22] The use of enzyme to catalyze thiol-norbornene click reaction also has the advantage of independent and modular controls over gelation kinetics and final gel properties. This is particularly important as gelation speed and final gel properties are often coupled together in conventional click hydrogels (i.e., higher macromer contents/functionalities are required for faster gelation, which leads to higher degree of gel crosslinking). To this end, horseradish peroxidase (HRP) has emerged as a highly useful enzyme for *in situ* crosslinking of hydroxyl-phenol (e.g., hydroxyphenylacetic acid (HPA), tyramine, or tyrosine) or vinyl-modified polymers into hydrogels.[23-25] HRP initiates hydrogel crosslinking by generating radical species in the

1  
2  
3 presence of hydrogen peroxide ( $H_2O_2$ ), which is provided either through exogenous addition or  
4 generated *in situ* through tandem enzymatic reactions (i.e., HRP with Glucose oxidase (GOX)  
5 and glucose).[26] For example, Kim *et al.* used HRP/GOX initiated crosslinking to form gelatin-  
6 based hydrogel with tunable mechanical property and gelation time.[27] These hydrogels also  
7 exhibited high cytocompatibility for encapsulation of human dermal fibroblasts. More recently,  
8 Gantumur and colleagues reported a crosslinking mechanism in which HRP was used as both  
9 the catalyst and the supplier of  $H_2O_2$ . [28] It was hypothesized that HRP oxidizes thiol moieties on  
10 itself to generate  $H_2O_2$ . This self-oxidization process was accelerated with high concentration of  
11 glucose and HRP. In addition to catalyzing crosslinking of hydroxyl-phenol-modified polymers into  
12 hydrogels, HRP was recently used to catalyze Reversible Addition-Fragmentation chain Transfer  
13 (RAFT) polymerization,[29] as well as thiol-allylether[22] and tetrazine-norbornene hydrogel  
14 crosslinking.[30] As demonstrated by Zavada *et al.*, PEG diallyl ether (PEGDAE) and ethoxylated  
15 trimethylolpropane tri(3-mercaptopropionate) (ETTMP) can be successfully crosslinked to form  
16 hydrogels with HRP and  $H_2O_2$ . [22] However, the gel points for HPR-initiated thiol-allylether  
17 gelation were on the order of 10 minutes using moderately high HRP concentrations (~100-300  
18 U/mL).[22] Nevertheless, HRP provides diverse routes for preparing hydrogels suitable for various  
19 biomedical applications. To the best of our knowledge, however, no prior study has utilized HRP  
20 or other enzyme to initiate the crosslinking of modular and dynamic thiol-norbornene hydrogels  
21 under ambient and aqueous conditions.

22  
23  
24 In this contribution, we present the use of HRP to initiate crosslinking of modular thiol-  
25 norbornene hydrogels. Differing from the crosslinking of hydroxyl-phenyl (e.g., tyramine)  
26 containing macromers into hydrogels, HPR-initiated thiol-norbornene hydrogelation exhibits  
27 characteristic modularity in hydrogel crosslinking. Specifically, we used 8-arm PEG-norbornene  
28 (PEG8NB) or gelatin-norbornene (GelNB) as the norbornene-modified macromers for  
29 crosslinking with multi-functional thiols (e.g., dithiothreitol (DTT), 4-arm PEG-thiol (PEG4SH), or  
30  
31  
32  
33  
34  
35  
36  
37  
38  
39  
40  
41  
42  
43  
44  
45  
46  
47  
48  
49  
50  
51  
52  
53  
54  
55  
56  
57  
58  
59  
60

1  
2  
3 bis-cysteine-bearing peptide) into step-growth hydrogels. H<sub>2</sub>O<sub>2</sub> needed for activating HRP was  
4 supplied either exogenously or generated *in situ* via GOX and glucose. In addition to studying the  
5 parameters critical for initiating enzymatic reaction, we examined the effect of tyrosine residue on  
6 crosslinking efficiency and post-gelation dynamic stiffening of PEG-peptide hydrogels. Similar to  
7 other HRP-based hydrogel crosslinking, the system exhibits high cytocompatibility for *in situ* cell  
8 encapsulation under proper reaction conditions. Finally, we explored the additional tyrosine  
9 residues on the peptide linker for enzyme-mediated dynamic gel stiffening.  
10  
11  
12  
13  
14  
15  
16  
17

## 18 **2. Material and Methods:**

### 19 *2.1 Materials*

20  
21  
22 8-arm poly(ethylene glycol) (PEG-OH) (20 kDa) was purchased from JenKem Technology;  
23 HRP (220 U/mg) and mushroom tyrosinase (MT, 845 U/mg) were purchased from Worthington.  
24 GOX (111 U/mg) was acquired from Amresco. All other chemicals were purchased from Fischer  
25 Scientific and used without further purification unless otherwise stated. 8-arm PEG-ester-  
26 norbornene (PEG8NB, ~95% substitution) and photoinitiator lithium aryl phosphinate (LAP) were  
27 synthesized as described previously.[5, 31, 32]  
28  
29  
30  
31  
32  
33  
34  
35

### 36 *2.2 Peptide synthesis and purification*

37  
38 All peptides were synthesized using standard solid-phase peptide synthesis in an  
39 automated microwave-assisted peptide synthesizer (CEM Liberty 1) using Fmoc-protected amino  
40 acids. Peptide cleavage was performed using a cleavage cocktail containing 7.6 mL trifluoroacetic  
41 acid (TFA), 0.2 mL triisopropylsilane (TIS), 400 mg phenol, and 0.2 mL double distilled water. The  
42 peptides were cleaved from the resin for ~3 h at room temperature and precipitated in cold ethyl  
43 ether. The cleaved peptides were dried *in vacuo* and purified by reverse phase HPLC  
44 (PerkinElmer Flexar system) using 95%/5% (v/v) water/acetonitrile with trace (0.1 vol.%) of TFA  
45 as the starting solvent mobile phase. A linear gradient of acetonitrile was used to separate the  
46 products through a semi-prep scale peptide C18 column at 5 mL/min flow rate. The separation  
47  
48  
49  
50  
51  
52  
53  
54  
55  
56  
57  
58  
59  
60

1  
2  
3 processes were monitored with a UV/vis detector at 280 nm (for peptides with tyrosine residue)  
4 or 220 nm (for peptides without tyrosine residue). Purified peptides were characterized with liquid  
5 chromatography coupled with mass spectrometry (Agilent Technologies, 1200 series LC/MS  
6 system).  
7  
8  
9

### 10 11 12 *2.3 Hydrogel fabrication*

13  
14 To fabricate HRP/H<sub>2</sub>O<sub>2</sub> mediated thiol-norbornene hydrogel, macromer PEG8NB was  
15 crosslinked with either DTT or bis-cysteine-bearing peptides (i.e. CGGGC, CYGGGYC,  
16 CGGYGGC, KCYGGYGGYCK). Specifically, to make a 1:1 thiol-to-norbornene ratio ( $R_{\text{thiol/ene}}=1$ )  
17 of PEG8NB-KCYGGYGGYCK hydrogel, 2.5 wt% of PEG8NB and 10 mM of KCYGGYGGYCK  
18 (final concentrations) were dissolved in phosphate buffer solution (PBS) at pH 7.4. HRP (1 U/ml)  
19 and H<sub>2</sub>O<sub>2</sub> (0.5 mM) were added to the solution, followed by vortexing for ~5 seconds. The  
20 precursor solution was immediately pipetted in between two glass slides separated by 1-mm-thick  
21 spacers. Gelation occurred within 5 minutes at room temperature. The hydrogels crosslinked from  
22 PEG8NB and tyrosine-free linker (CGGGC or DTT) or with GelNB and PEG4SH were also  
23 prepared following the same procedure but with a more concentrated HRP (100 to 200 U/ml).  
24  
25  
26  
27  
28  
29  
30  
31  
32  
33  
34

35 For dual enzyme (HRP/GOX)-mediated gelation, PEG8NB-DTT and PEG8NB-peptide  
36 hydrogels were prepared following the similar procedures described above. Briefly, 3 wt%  
37 PEG8NB and 12 mM (final concentrations) DTT or peptides were dissolved in PBS with 1 U/ml  
38 (for tyrosine-containing peptides), or 200 U/ml HRP (for CGGGC or DTT), 1 U/ml GOX, and 10  
39 mM glucose. The solution was vortexed for ~5 seconds before pipetted in a Teflon mold with 8-  
40 mm diameter cavities. Hydrogel discs were obtained after 5 minutes of gelation.  
41  
42  
43  
44  
45  
46  
47

48 To stiffen hydrogels using mushroom tyrosinase (MT), PEG8NB hydrogels were  
49 crosslinked by tyrosine-containing peptide (thiol to norbornene ratio was fixed at 1). Prior to MT-  
50 mediated stiffening, hydrogels were swollen in PBS for 24 hrs to wash off un-crosslinked species.  
51 To induce dynamic stiffening, hydrogels were submerged in 1 kU/ml MT for 6 hrs. Afterwards, MT  
52  
53  
54  
55  
56  
57  
58  
59  
60

1  
2  
3 was removed via swelling hydrogels in PBS for 24 hrs, followed by rheological measurements of  
4 hydrogel shear modulus.  
5  
6

#### 7 8 *2.4 Rheometry* 9

10 Rheological measurements were conducted with circular hydrogel discs fabricated  
11 between two glass slides. Gel discs were punched out with an 8 mm biopsy punch. The hydrogels  
12 were carefully transferred to the rheometer platform prior to initiating the measurements. Storage  
13 and loss moduli ( $G'$  and  $G''$ ) of the hydrogels were determined using a Bohlin CVO 100 digital  
14 rheometer fitted with an 8-mm diameter parallel geometry. Frequency sweep was first performed  
15 to determine the frequency at which the viscoelastic properties are independent of the imposed  
16 stress or strain (i.e., linear viscoelastic (LVE) region). For most covalently crosslinked hydrogels,  
17 a frequency of 1 Hz typically falls within the LVE region. The rheological measurements were  
18 performed in strain-sweep mode with the strain ranging from 0.1% to 5%, and the oscillation  
19 frequency was kept constant at 1 Hz.  
20  
21  
22  
23  
24  
25  
26  
27  
28  
29  
30

31 For *in situ* gelation experiments, precursor PEG8NB solution containing thiol crosslinkers,  
32 HRP,  $H_2O_2$  (or GOX and glucose) were mixed and vortexed for 5 seconds. Immediately after  
33 vortexing, 7  $\mu$ L of the mixture was placed on the lower plate and the geometry was lowered to 90  
34  $\mu$ m. A layer of mineral oil was applied on the edge of the plate geometry head to prevent  
35 dehydration.  
36  
37  
38  
39  
40  
41

#### 42 *2.5 Norbornene and Thiol Consumption* 43

44 The thiol conversion study was conducted with precursor solutions containing linear  
45 PEGNB, DTT, HRP and  $H_2O_2$ . Briefly, 3.5 wt% PEGNB, 14 mM DTT, 200 U/ml HRP, and 1.5 mM  
46 of  $H_2O_2$  were mixed together and portions of the solution (25  $\mu$ L) were collected immediately after  
47 mixing and at intervals of every 2 minutes afterward. Remaining thiol contents were determined  
48 using Ellman's reagent (5,5-dithio-bis-(2-nitrobenzoic acid. ThermoFisher Scientific) following the  
49  
50  
51  
52  
53  
54  
55  
56  
57  
58  
59  
60

1  
2  
3 manufacturer's protocol. The thiol concentration left at each specific time point was used to  
4  
5 calculate the amount of thiol that had been consumed.  
6

7  
8 As for norbornene consumption, mixtures of linear PEGNB, DTT, HRP, H<sub>2</sub>O<sub>2</sub> at different  
9  
10 thiol to norbornene ratios (keeping PEGNB concentration constant at 3.5 wt%) were mixed in  
11  
12 deuterium oxide for 10 minutes. Polymer samples for <sup>1</sup>H NMR analysis were prepared at a  
13  
14 concentration of 20 mg/ml. The reaction mixtures were then subjected to analysis using Bruker  
15  
16 Avance III 500 Hz NMR. The amount of norbornene left after the reaction for each R<sub>thiol/ene</sub> ratio  
17  
18 was calculated using the ratio of the integration of the norbornene peaks at 6.00 to 6.36 ppm over  
19  
20 the integration of the PEG backbone region from 4.21 – 4.37 ppm.  
21

## 22 23 *2.6 Characterization of gel fraction*

24  
25 Hydrogels were formed with PEG8NB, DTT, HRP and H<sub>2</sub>O<sub>2</sub> (or GOX/glucose); each gel  
26  
27 was prepared from 45 μL of precursor solution. Immediately after gelation, hydrogels were dried  
28  
29 in vacuo and weighed to obtain first dried weight (W<sub>1st dried</sub>). The dried gels were incubated in  
30  
31 ddH<sub>2</sub>O at 37 °C overnight to remove un-crosslinked species. Afterwards, swollen weights were  
32  
33 obtained; swollen gels were dried and weighed again to obtain the second dried weight (W<sub>2nd dried</sub>).  
34  
35 Gel fraction (**Equation 1**) was determined by the ratio of the 2<sup>nd</sup> dried weight over the 1<sup>st</sup> dried  
36  
37 weight:  
38

$$39 \text{ Gel fraction} = \frac{W_{2nd \text{ dried}}}{W_{1st \text{ dried}}} \quad (1)$$

40  
41  
42  
43 Hydrogel mass swelling ratios (q, **Equation 2**) were calculated using the following equation:  
44

$$45 q = \frac{W_{swollen}}{W_{2nd \text{ dried}}} \quad (2)$$

## 46 47 *2.7 In-gel oxygen measurements*

48  
49  
50 A needle-type oxygen probe connected to Microx4 oxygen sensor (PreSens Precision  
51  
52 Sensing GmbH) was used to obtain the oxygen concentrations within the gels. The needle of the  
53  
54 oxygen probe was inserted into the gel at specified time points. After needle penetration, the  
55  
56  
57



1  
2  
3 optical fiber of the probe was extended to the tip of the needle so that it was exposed to the gel  
4  
5 but remained housed within the needle.  
6

### 7 8 *2.8 NIH/3T3 fibroblast encapsulation*

9  
10 Cytocompatibility of the enzymatically crosslinked thiol-norbornene hydrogel was evaluated  
11 using murine NIH/3T3 fibroblasts acquired from American Type Culture Collection (ATCC). Cells  
12 were maintained in high glucose Dulbecco's modified eagle medium (DMEM) containing 10%  
13 fetal bovine serum and 1% penicillin-streptomycin before performing cell encapsulation. All  
14 macromer components used for cell encapsulation were sterilized by passing through sterile 0.22  
15  $\mu\text{m}$  syringe filter. For cell encapsulation, a solution of 3 wt% PEG8NB, 13 mM KCYGGYGGYCK  
16 peptide, 1 mM CRGDS peptide, 1 U/ml HRP, and 0.5 mM  $\text{H}_2\text{O}_2$  were mixed together, followed by  
17 gently suspending NIH/3T3 cells into the precursor solution (final cell density:  $2 \times 10^6$  cells/ml).  
18 The mixture was then added to 1 mL syringes (with the top cut open) and allowed to gel for 5  
19 minutes. After that, cell-laden gels were transferred into a 24-well plate. GelNB-PEG4SH cell-  
20 laden hydrogels were prepared following similar steps but with a higher HRP concentration (100  
21 U/ml) and without the addition of CRGDS. To evaluate cell viability after encapsulation and  
22 throughout culturing period, the encapsulated cells were stained with NucBlue®, which labels  
23 nuclei of all cells, and NucGreen®, which stains cells with compromised plasma membranes (i.e.,  
24 dead cells). The numbers of live (all cells minus dead cells) and dead cells were imaged with a  
25 confocal microscope and counted using ImageJ software.  
26  
27  
28  
29  
30  
31  
32  
33  
34  
35  
36  
37  
38  
39  
40  
41  
42  
43

### 44 *2.9 Dynamic stiffening of enzymatically crosslinked PEG-peptide hydrogels*

45  
46 MT were used to induce dynamic stiffening of PEG8NB-peptide hydrogels. 24 hrs after  
47 cell encapsulation, the gels were incubated in 1 kU/ml MT for 6 hours to induce stiffening.  
48 Afterwards the enzyme was removed via swelling in culture media for 24 hrs. To observe the  
49 effect of matrix stiffening on cell morphology and cytoskeletal organization, cell-laden hydrogels  
50 were fixed and stained for cell nuclei and F-actin. Specifically, at predetermined time points after  
51  
52  
53  
54  
55  
56  
57  
58  
59  
60

1  
2  
3 encapsulation, cell-laden hydrogels were fixed with 4% paraformaldehyde and permeabilized  
4 with saponin solution following a published protocol.[33, 34] Next, rhodamine phalloidin and DAPI  
5 were used to stain for F-actin and nuclei, respectively. Live/Dead and immunofluorescence  
6 stained samples were imaged with Olympus Fluoview FV100 laser scanning microscopy.  
7 Live/Dead images were captured at 10x objective, with Z-stacked of 10 slices and 10  $\mu\text{m}$  per slice.  
8 Immunofluorescence images were captured at 20x objective, with Z-stacked of 10 slices and 2  
9  $\mu\text{m}$  per slice.

## 18 2.10 Statistics

20 All experiments were performed independently for three times and with a minimum of three  
21 samples per conditions. Statistical significance was evaluated using a two-tail t-test in Prism 5  
22 software. Single, double, and triple asterisks represent  $p < 0.05$ , 0.01, and 0.001 respectively.  
23  
24  
25  
26

## 27 3. Results and Discussion

### 29 3.1 Characterization of HRP-mediated thiol-norbornene gelation

31 While HRP has been previously used to initiated crosslinking of thiol-allylether  
32 hydrogels,[22] its utility on initiating thiol-norbornene gelation has not been reported. We reasoned  
33 that thiyl radicals generated by HRP can propagate to the strained norbornene bond, creating a  
34 carbon-center radical to abstract hydrogen from another thiol group. A stable thioether bond is  
35 subsequently formed, thus completing the step-growth cycle (**Fig. 1A**). To test this hypothesis,  
36 we first mixed PEG8NB (20 kDa), DTT, HRP, and  $\text{H}_2\text{O}_2$  in test tubes and evaluated gelation speed  
37 using a simple tilt-test. As shown in **Fig. 1B**, gelation occurred within a few minutes only when all  
38 four components (PEG8NB, DTT, HRP,  $\text{H}_2\text{O}_2$ ) were included. The crosslinking was clearly  
39 triggered by enzymatic reaction because gelation did not occur without HPR or  $\text{H}_2\text{O}_2$ .  
40 Furthermore, gelation was not due to norbornene homo-polymerization (i.e., no DTT) or entirely  
41 by HRP-mediated disulfide bond formation (i.e., no PEG8NB groups). To ensure that gelation was  
42 a result of HRP-mediated thiol-norbornene reaction, we performed thiol and norbornene  
43  
44  
45  
46  
47  
48  
49  
50  
51  
52  
53  
54  
55  
56  
57  
58  
59  
60

1  
2  
3 consumption tests using linear PEGNB, DTT, HRP, and H<sub>2</sub>O<sub>2</sub>. Linear PEGNB was used to prevent  
4 crosslinking while permitting solution-based assay since not all formulations formed hydrogels,  
5 especially at early reaction time points (in thiol consumption test) and low thiol/ene ratios (in  
6 norbornene consumption test). **Fig. 1C** shows that a time-dependent depletion of thiols only  
7 occurred in the presence of all necessary components (i.e., PEGNB, DTT, and HRP/H<sub>2</sub>O<sub>2</sub>).  
8 Limited thiol consumption (~30%) was detected in the presence of DTT and HRP, which could be  
9 attributed to HRP-catalyzed disulfide bond formation. It should be noted that, in the absence of  
10 HRP, no thiol consumption was detected (**Fig. 1C. No HRP group**), suggesting that un-catalyzed  
11 disulfide bond formation was not a concern within the 15 minutes reaction time.

12  
13  
14  
15  
16  
17  
18  
19  
20  
21  
22 Using proton NMR, we analyzed chemical shifts of norbornene group (**Fig. 1D**) and  
23 established a linear and quantitative relationship of norbornene consumption as a function of thiol-  
24 to-norbornene ratio ( $R_{\text{thiol/ene}}$ ). It is worth noting that there was an incomplete norbornene  
25 consumption even when  $R_{\text{thiol/ene}}$  reached unity. The lower than expected and incomplete  
26 norbornene consumption could be a result of the HRP reactivity towards thiol groups (**Fig 1C. No**  
27 PEGNB group). Since the  $R_{\text{thiol/ene}}$  values were calculated based on the amounts of thiol and  
28 norbornene groups added in the solutions, partial consumption of thiol by HRP would reduce the  
29 actual thiol-to-norbornene ratio, which could explain why a lower than expected norbornene  
30 consumption was obtained.

31  
32  
33  
34  
35  
36  
37  
38  
39  
40  
41 Using *in situ* rheometry, we demonstrated a rapid gelation kinetics, which was on par with  
42 the visible light initiated thiol-norbornene gelation system (gel point ~80 s, **Fig. 2A**).<sup>[16]</sup> Enzymatic  
43 crosslinking of DTT and PEG8NB into hydrogels required relatively low concentration of HRP  
44 (~100 U/mL, **Fig. 2B**) and H<sub>2</sub>O<sub>2</sub> (~0.5 mM, **Fig. 2C**). Through adjusting PEG8NB macromer  
45 contents (i.e., 3.5, 4, and 4.5 wt%), gel crosslinking density and modulus ( $G' \sim 1$  to 3 kPa, **Fig.**  
46 **2D**) could be readily tuned in a range relevant to many normal and diseased tissues, including  
47 stem cell differentiation,<sup>[35-37]</sup> tumor progression,<sup>[34, 38-41]</sup> and fibrosis.<sup>[42, 43]</sup> More  
48 importantly, unlike light-mediated photochemistry that has light attenuation issue, especially in  
49  
50  
51  
52  
53  
54  
55  
56  
57

1  
2  
3 dark samples, we showed that HRP-catalyzed thiol-norbornene hydrogels can be used to form  
4 hydrogels with higher depth/thickness since enzymatic reactions occurs simultaneously  
5 throughout the dimension of the vessel (**Fig. 2E**). Thiol-norbornene hydrogels crosslinked by the  
6 HRP/H<sub>2</sub>O<sub>2</sub> system also appeared to maintain good fidelity of the syringe mold. In principle, this  
7 enzymatic crosslinking scheme can be adapted for injectable delivery of thiol-norbornene  
8 hydrogels, which have an ideal network structure and can conform the size and shape of the  
9 delivery site.  
10  
11  
12  
13  
14  
15  
16  
17

### 18 *3.2 Tyrosine-assisted enzymatic crosslinking of PEG-peptide hydrogels*

19  
20 After demonstrating the feasibility of HRP-initiated thiol-norbornene hydrogel crosslinking  
21 using DTT as a crosslinker, we asked if bis-cysteine peptide linkers can be used to form PEG-  
22 peptide hydrogels. Peptide crosslinkers are advantageous in promoting cell fate processes, such  
23 as protease-mediated matrix cleavage. As a proof-of-concept, we designed a model peptide linker  
24 containing only terminal cysteines and internal glycine residues (i.e., CGGGC) and tested gelation  
25 under 1 mM H<sub>2</sub>O<sub>2</sub> and a range of HRP concentrations (i.e., 1 to 200 U/mL). While gelation  
26 occurred at high HRP concentrations (100-200 U/mL) as expected, no sol-gel transition was  
27 observed when HRP concentration was lower to 5 U/mL even after 30 minutes (data not shown).  
28 We then examined whether adding soluble tyrosine could promote HRP-mediated thiol-  
29 norbornene gelation as this approach was reported to improve HRP-induced crosslinking of  
30 thiolated polymers,[44] as well as the gelation efficiency of photopolymerized thiol-norbornene  
31 hydrogels.[45] Unfortunately, soluble tyrosine also did not assist thiol-norbornene PEG-peptide  
32 gelation using 5 U/mL HRP (data not shown).  
33  
34  
35  
36  
37  
38  
39  
40  
41  
42  
43  
44  
45  
46  
47

48 We next tested whether placing tyrosine residue on the cysteine-containing peptide linkers  
49 would enhance HRP-mediated thiol radical generation. This approach was inspired by another  
50 recent work where tyrosine/cysteine dually labeled protein was used to facilitate HRP-mediated  
51 di-thiol crosslinks formation.[46] **Fig. 3A** illustrates the potential mechanism of tyrosine-assisted  
52  
53  
54  
55  
56  
57  
58  
59  
60

1  
2  
3 thiyl radical generation. Experimentally, we used a tyrosine containing model peptide CYGGGYC  
4  
5 for HRP-mediated thiol-norbornene gelation tests. Surprisingly, immediate gelation was obtained  
6  
7 at 5 U/mL HRP and 1 mM H<sub>2</sub>O<sub>2</sub>, suggesting that adding tyrosine residues on the peptide sequence  
8  
9 improved thiyl radical generation and hence thiol-norbornene gelation. It is worth noting that  
10  
11 gelation was not due to HRP-mediated di-tyrosine crosslinking or norbornene-tyrosine reaction,  
12  
13 as control experiments using a cysteine-free peptide (i.e., KGYGGYGGYGK) did not yield  
14  
15 hydrogel crosslinking (data not shown). In order to obtain gelation in a more manageable  
16  
17 timeframe, we intentionally reduced the concentration of HRP and H<sub>2</sub>O<sub>2</sub> to 1 U/mL and 0.5 mM,  
18  
19 respectively. Under these conditions, PEG-peptide thiol-norbornene hydrogels could be  
20  
21 crosslinked within 10 minutes and shear moduli of these hydrogels (as characterized by strain-  
22  
23 sweep rheometry) were higher when using peptide linker containing more tyrosine residues (**Fig.**  
24  
25 **3B**). Additional gelation tests using off-stoichiometric ratios of thiol/norbornene led to gels with  
26  
27 tunable moduli (**Fig. 3C**), a typical characteristic of modularly crosslinked PEG-peptide thiol-  
28  
29 norbornene hydrogels. It should also be noted that the above results were obtained without  
30  
31 altering the concentrations of PEG8NB macromer (i.e., 3 wt%), HRP (i.e., 1 U/mL), or H<sub>2</sub>O<sub>2</sub> (i.e.,  
32  
33 0.5 mM), further providing flexibility in preparing hydrogels with highly tunable properties.  
34  
35

### 3.3 HRP/GOX dual enzymatic thiol-norbornene gelation

36  
37  
38  
39 Next, we explored whether thiol-norbornene gelation could be achieved using enzyme-  
40  
41 catalyzed tandem reactions. Specifically, H<sub>2</sub>O<sub>2</sub> needed for HRP-catalyzed thiol-norbornene  
42  
43 gelation was generated in tandem by GOX, glucose, and dissolved oxygen (**Fig. 4A**). Gelation of  
44  
45 PEG8NB and CYGGGYC peptide using this scheme was successful and the degree of hydrogel  
46  
47 crosslinking was dose-dependently and almost linearly tuned in the presence of 1 to 10 mM  
48  
49 glucose (**Fig. 4B**). However, when glucose concentration was raised to above 10 mM, hydrogels  
50  
51 were formed with lower moduli, suggesting a reduced crosslinking efficiency. This was likely due  
52  
53 to an inhibition effect of higher H<sub>2</sub>O<sub>2</sub> to HRP and/or GOX (i.e., more H<sub>2</sub>O<sub>2</sub> would be generated at  
54  
55  
56  
57  
58  
59  
60

1  
2  
3 higher glucose concentrations).[47, 48] We further compared crosslinking efficiency of enzymatic  
4 thiol-norbornene hydrogels to that of UV crosslinked gels with the same macromer compositions.  
5 In terms of gel fraction (**Fig. 4C**), hydrogels crosslinked by the HRP/GOX/glucose system ( $87.4 \pm$   
6  $2.1$ ) were comparable to that of UV crosslinked gels ( $87.8 \pm 2.4$ ), suggesting high crosslinking  
7 efficiency of the HRP-mediated thiol-norbornene reactions. However, when gels were crosslinked  
8 by the HRP/H<sub>2</sub>O<sub>2</sub> system, a slightly lower gel fraction ( $77.5 \pm 1.0$ ) was obtained, which could be  
9 attributed to HRP inactivation caused by bolus addition of H<sub>2</sub>O<sub>2</sub>. [49-51] Further characterizations  
10 of mass swelling ratio ( $q$ ) and shear modulus ( $G'$ ) of the hydrogels confirmed a lower crosslinking  
11 efficiency in gels formed by the HRP/H<sub>2</sub>O<sub>2</sub> system when comparing to gels formed by HRP/GOX  
12 tandem enzymatic reactions (i.e., higher  $q$  and lower  $G'$  **Fig. 4D**).

23  
24 To gain insights into the effect of tandem HRP/GOX enzymatic thiol-norbornene reactions  
25 on the oxygen contents during gelation, we used a needle-type oxygen probe to detect  
26 concentrations of dissolved oxygen inside the two groups of hydrogels at various time points post-  
27 gelation (0-24 hr). Hydrogels were placed in PBS immediately after gelation. As shown in **Fig. 4E**,  
28 oxygen contents inside the hydrogels formed by HRP/H<sub>2</sub>O<sub>2</sub>-initiated gelation remained close to  
29 normoxia after gelation. This is not surprising, as no dissolved oxygen was needed in HRP/H<sub>2</sub>O<sub>2</sub>-  
30 mediated reaction. However, in the HRP/GOX/glucose gelation system, severe hypoxia (~ 1%)  
31 was detected within one hour post-gelation. After 5 hours, O<sub>2</sub> content in hydrogel increased to  
32 ~6%. Oxygen level in the hydrogel returned to almost normoxia after 24 hours, presumably due  
33 to oxygen diffusion into the gel over time. The increased 'in-gel oxygen' results suggested that no  
34 GOX was permanently trapped in the hydrogel after crosslinking. The highly efficient enzyme-  
35 initiated PEG-peptide thiol-norbornene hydrogel system is advantageous as injectable cell-  
36 responsive matrices for tissue engineering applications. Furthermore, the transient hypoxia  
37 occurred within the dual enzyme-crosslinked thiol-norbornene hydrogels may be exploited to  
38  
39  
40  
41  
42  
43  
44  
45  
46  
47  
48  
49  
50  
51  
52  
53  
54  
55  
56  
57  
58  
59  
60

1  
2  
3 improve 3D vascularization and cytokine secretion from mesenchymal stem cells in the future.[52,  
4  
5 53]

### 8 *3.4 Enzymatically crosslinked gelatin-based thiol-norbornene hydrogels*

9  
10 To demonstrate the versatility of the HRP mediated gelation, hydrogels were formed with  
11 norbornene-modified gelatin (GelNB),[54] an attractive macromer used extensively in many  
12 biomedical applications due to its intrinsic biocompatibility and degradability.[39, 55-57] Because  
13 GelNB and PEG4SH were both multifunctional macromers, HRP concentration was lowered to  
14 ~100 U/ml (instead of 200 U/ml for PEG8NB) to achieve a more manageable gelation time. GelNB  
15 and PEG4SH readily crosslinked into hydrogels with highly tunable stiffness. Gel moduli were  
16 controlled by adjusting either gelatin content (**Fig. 5A**) or thiol to norbornene ratio (**Fig. 5B**).  
17 Hypothetically, GOX/glucose system is more ideal for cell encapsulation because GOX-generated  
18  $H_2O_2$  would be consumed by HRP soon after its production. On the other hand, exogenously  
19 added  $H_2O_2$  would present a much higher initial  $H_2O_2$  concentration for the encapsulated cells.  
20 However, the in-gel oxygen measurements results shown in **Fig. 4C** demonstrated an extremely  
21 low oxygen level within the first hour of gelation (<1%), which might not be ideal for cells survival.  
22 Other potential challenges with the HRP/GOX/glucose system as a mean to supply  $H_2O_2$  lie in the  
23 fact that the remaining GOX within the hydrogel can continuously consume glucose within the  
24 culture media to generate gluconic acid. In addition, the remaining HRP, GOX and glucose could  
25 also crosslink the pH indicator phenol red in the media, which may hinder its buffering effect on  
26 pH changes. Therefore, we chose HRP/ $H_2O_2$  system for cell encapsulation studies. To minimize  
27 potential cytotoxicity,  $H_2O_2$  concentration was lowered to 0.5 mM. A recent study on HRP/ $H_2O_2$   
28 enzymatic reaction reported by Park *et al.* has concluded that any initial  $H_2O_2$  concentration below  
29 0.063 wt% (~18 mM) is a safe level for cell culture and almost all residual  $H_2O_2$  would be converted  
30 to water and oxygen by HRP.[58] By quantifying the numbers of live and dead cells using live/dead  
31 staining and confocal imaging, we found that enzymatically crosslinked GelNB-PEG4SH  
32  
33  
34  
35  
36  
37  
38  
39  
40  
41  
42  
43  
44  
45  
46  
47  
48  
49  
50  
51  
52  
53  
54  
55  
56  
57  
58  
59  
60

1  
2  
3 hydrogels displayed good cytocompatibility with above 85% of the encapsulated cells remained  
4 alive after 24 hours of encapsulation (**Fig. 5C**). Moreover, encapsulated cells proliferated  
5 significantly after 8 days of culture (**Fig. 5D**). Since gelatin is susceptible to protease-mediated  
6 degradation, the encapsulated cells were able to form extensive and interconnected network  
7 following local matrix degradation. All in all, the enzymatically crosslinked GeINB-PEG4SH  
8 hydrogels are capable of supporting long term cell survival as well as providing favorable platform  
9 for cell expanding and proliferation.  
10  
11  
12  
13  
14  
15  
16  
17

### 18 *3.5 Dynamic stiffening of enzymatically crosslinked PEG-peptide hydrogels*

19

20 **Fig. 3** has clearly shown that tyrosine residues on bis-cysteine peptide linker facilitate thiyl  
21 radical generation and thiol-norbornene hydrogel crosslinking. One potential mechanism  
22 responsible for this gelation is that the hydroxyl and thiol groups are in close proximity on the  
23 peptide linker. It is likely that the hydroxyl group on tyrosine residue regains its hydrogen atom  
24 following thiyl radical generation (**Fig. 2A**). We then asked if hydroxyl side group on tyrosine  
25 residues can be exploited for mushroom tyrosinase (MT)-mediated post-gelation dynamic  
26 stiffening (**Fig. 6A**). We have previously developed similar strategies to dynamically stiffen PEG-  
27 peptide hydrogels for controlling cell fate processes.[39, 40] We found that the enzymatically  
28 crosslinked thiol-norbornene PEG-peptide hydrogels could indeed be dynamically stiffened using  
29 exogenously added MT (incubation for 6 hours. **Fig. 6B, 6C**), suggesting that the hydroxyl-phenol  
30 groups on tyrosine remained protonated following HRP-mediated gelation. Upon the addition of  
31 MT, these tyrosine residues were catalyzed to DOPA dimers that exhibit characteristic  
32 yellow/brown color as shown in **Fig. 6B**. [33, 39, 40] These additional DOPA dimers resulted in  
33 increased gel crosslinking density and shear modulus (**Fig. 6C**). Enzymatic stiffening occurred in  
34 hydrogels crosslinked by peptides with two or three tyrosine residues, as well as gels crosslinked  
35 with HRP/H<sub>2</sub>O<sub>2</sub> or HRP/GOX/glucose systems. Most importantly, the degrees of stiffening (from  
36 2 to 5 kPa) were relevant to the mechanics of many normal and diseased tissues.[59-62]  
37  
38  
39  
40  
41  
42  
43  
44  
45  
46  
47  
48  
49  
50  
51  
52  
53  
54  
55  
56  
57  
58  
59  
60



### 3.6 Cell encapsulation and dynamic stiffening of cell-laden hydrogels

Fibroblast has been known to play a critical role during normal wound healing, where the stiffness of the ECM increases significantly.[63] Our enzyme-mediated matrix stiffening strategy can be used to mimic this process and examine how matrix stiffening would regulate fibroblasts behavior. To investigate how dynamic stiffening affects cell fate, we encapsulated NIH/3T3 fibroblasts in PEG8NB-peptide hydrogels, with the peptide crosslinkers susceptible to mushroom tyrosinase (MT)-mediated on-demand stiffening. The PEG8NB-peptide hydrogels were divided into two groups: the control group, which received no MT treatment and the stiffened group, which underwent dynamic stiffening (i.e., treated with 1 kU/ml MT for 6 hours). Live/dead staining results show that both groups displayed good cytocompatibility, with 90% or more cell survived the enzymatic encapsulation process. (**Fig. 6D**). On day 1, the cells exhibited rounded morphology in both groups (**Fig. 6E**). However, after 8 days of culturing, immunofluorescence staining results show distinct differences in cell morphology between the soft and stiffened hydrogels. While cells cultured in the non-treated (or soft) gels exhibited extensive and significant cell spreading with many cells connected to each other, those in the stiffened hydrogels remained mostly as single cells. The extensive spreading in the soft group was similar to that observed in cells encapsulated within soft GelNB-PEG4SH gels (**Fig. 5D**). On the other hand, while the PEG8NB-peptide hydrogels used here did not contain protease-sensitive linkers, some cells in the stiffened gels still exhibited spreading and/or irregular protrusions after 8 days of culture (**Fig. 6E**). We reasoned that these cell protrusions were permitted by network defects and/or gradual hydrolysis of ester bonds located between the norbornene moiety and the PEG backbone. We have previously shown that hydrolysis of ester bonds in gels composed of 'PEG-ester-NB' macromer encouraged a higher degree of cell spreading when compared with gels formed by 'PEG-amide-NB'. [64] Nonetheless, these results suggested that soft gels exhibited appropriate mechanical strength to allow for more cell spreading. Due to the additional di-tyrosine crosslinks within the stiffened gels network, the mesh sizes of these hydrogels were smaller and could impose physical strain to

1  
2  
3 restrict gel degradation and cell spreading. This behavior is likely not exclusive to NIH/3T3 cells,  
4  
5 our result agreed with previous studies where soft gels were also shown to allow more spreading  
6  
7 than stiffened ones.[39] It is also important to note that, the minimal cell spreading behavior within  
8  
9 the stiffened group was mainly due to matrix stiffening and not due to cell death, because  
10  
11 pronounced increase in cell density were seen in both groups after 8 days. Cell density increase  
12  
13 indicated that NIH/3T3 fibroblasts were viable and able to proliferate even in stiffened hydrogels.  
14  
15 While we did not perform rheological measurements for cell-laden hydrogels, all hydrogels  
16  
17 underwent MT-mediated stiffening changed their color to dark brown (data not shown. Similar to  
18  
19 **Fig. 6B**), indicating that the gels were indeed stiffened. Future studies may be conducted to  
20  
21 correlate the degree of enzymatic matrix stiffening and mechanotransduction in the encapsulated  
22  
23 cells. Nonetheless, our stiffening experiments (**Fig. 6**) have also shown that the tyrosine residues not  
24  
25 only facilitated HRP-mediated thiol-norbornene gel crosslinking, but were also available for MT-  
26  
27 mediated stiffening to dynamically affect cell fate processes.  
28  
29

30  
31 Another important issue to note is that cell viability was slightly lower in the GelNB-  
32  
33 PEG4SH gels (**Fig. 5C**) than in the PEG-peptide gels. We reasoned that this was due to the  
34  
35 higher concentration of HRP used (i.e., 100 U/mL for GelNB-PEG4SH gels and 1 U/mL for PEG-  
36  
37 peptide gels) during encapsulation process, which could have adverse effect on fibroblasts.  
38  
39 Although less likely, the differences in radical generation mechanism of the HRP-mediated thiol-  
40  
41 norbornene system with and without the incorporation of tyrosine residues could also be a reason  
42  
43 for the viability discrepancy. Regardless of the macromers used, we have shown that cell-laden  
44  
45 thiol-norbornene hydrogels could be readily crosslinked enzymatically via HRP. Uniquely, the  
46  
47 PEG8NB-peptide hydrogel system exhibited additional dynamic and enzymatic stiffening feature  
48  
49 that has not been reported in other HRP-crosslinked gels. If desired, these tyrosine residues can  
50  
51 be explored for labeling/patterning of receptor binding ligands, a strategy reported recently by our  
52  
53 group.[33] Overall, the enzymatically crosslinked thiol-norbornene hydrogels address the  
54  
55 limitation of light attenuation issue in photopolymerization while retaining the modularity of the  
56  
57

1  
2  
3 thiol-norbornene crosslinking. The enzyme-mediated crosslinking mechanism can be utilized in a  
4 wide range of applications ranging from injectable cell-laden hydrogels to *in vitro* dynamic cell  
5 culture platforms.  
6  
7  
8  
9

#### 10 **4. Conclusion**

11  
12 In summary, we have developed the first orthogonal enzymatic thiol-norbornene click  
13 reaction suitable for forming modularly crosslinked hydrogels under ambient conditions.  
14 Furthermore, we discovered that HRP can be used to initiate gelation of macromers other than  
15 those containing hydroxyl-phenyl groups. Most importantly, the hydrogels can be dynamically  
16 stiffened by means of tyrosinase-mediated crosslinking owing to the preservation of tyrosine  
17 residues following the initial thiol-norbornene click gel reaction. The modular and dynamic  
18 hydrogels described in this contribution offer researchers an attractive alternative to form  
19 modularly crosslink and dynamic hydrogels without the concerns of light attenuation in thick  
20 samples or potential cell damage caused by UV light irradiation.  
21  
22  
23  
24  
25  
26  
27  
28  
29  
30

#### 31 **Acknowledgement**

32  
33 This project was supported in part by the Division of Materials Research (DMR) at the National  
34 Science Foundation (CAREER Award #1452390) and the National Cancer Institute (NCI) at the  
35 National Institutes of Health (NIH, R01CA227737).  
36  
37  
38  
39  
40  
41  
42  
43  
44  
45  
46  
47  
48  
49  
50  
51  
52  
53  
54  
55  
56  
57  
58  
59  
60

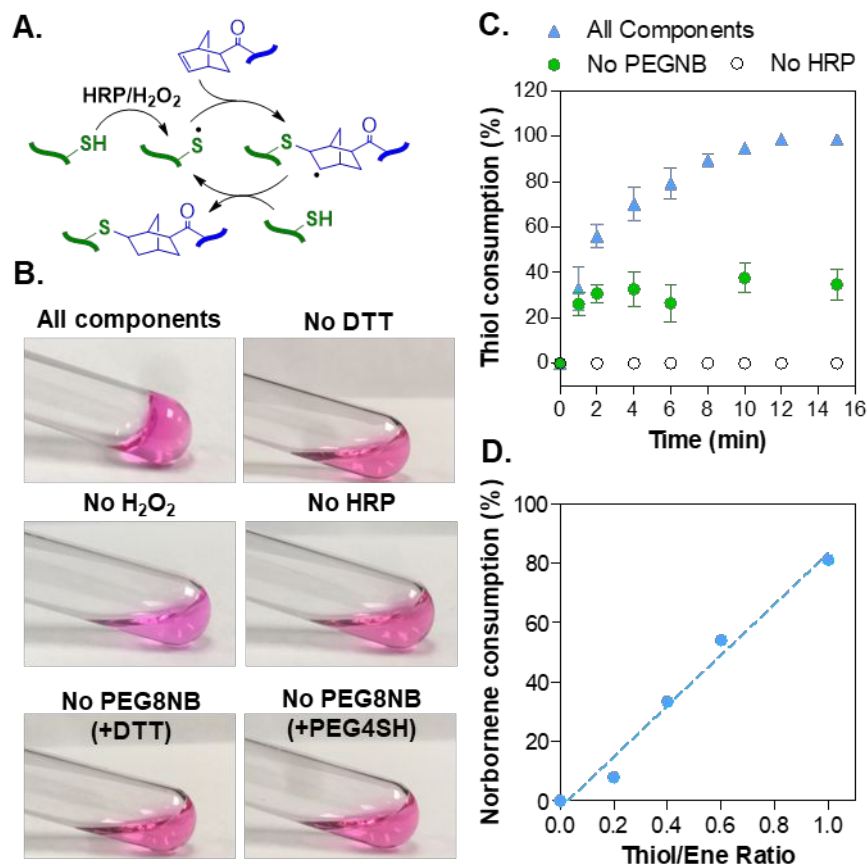


**Figure 1. HRP-mediated crosslinking of thiol-norbornene click reactions.** (A) Schematic of HRP/H<sub>2</sub>O<sub>2</sub>-induced thiyl radical generation and subsequent thiol-norbornene crosslinking. (B) Gelation tilt-test. All components: 200 U/mL HRP, 0.5 mM H<sub>2</sub>O<sub>2</sub>, 3.5 wt% PEG8NB, and 14 mM DTT. (C) Thiol consumption as a function of reaction time. (D) Norbornene consumption as a function of thiol-norbornene ratio (i.e., Thiol/Ene Ratio, calculated using the actual molarity of thiol and norbornene groups added to the reactions).

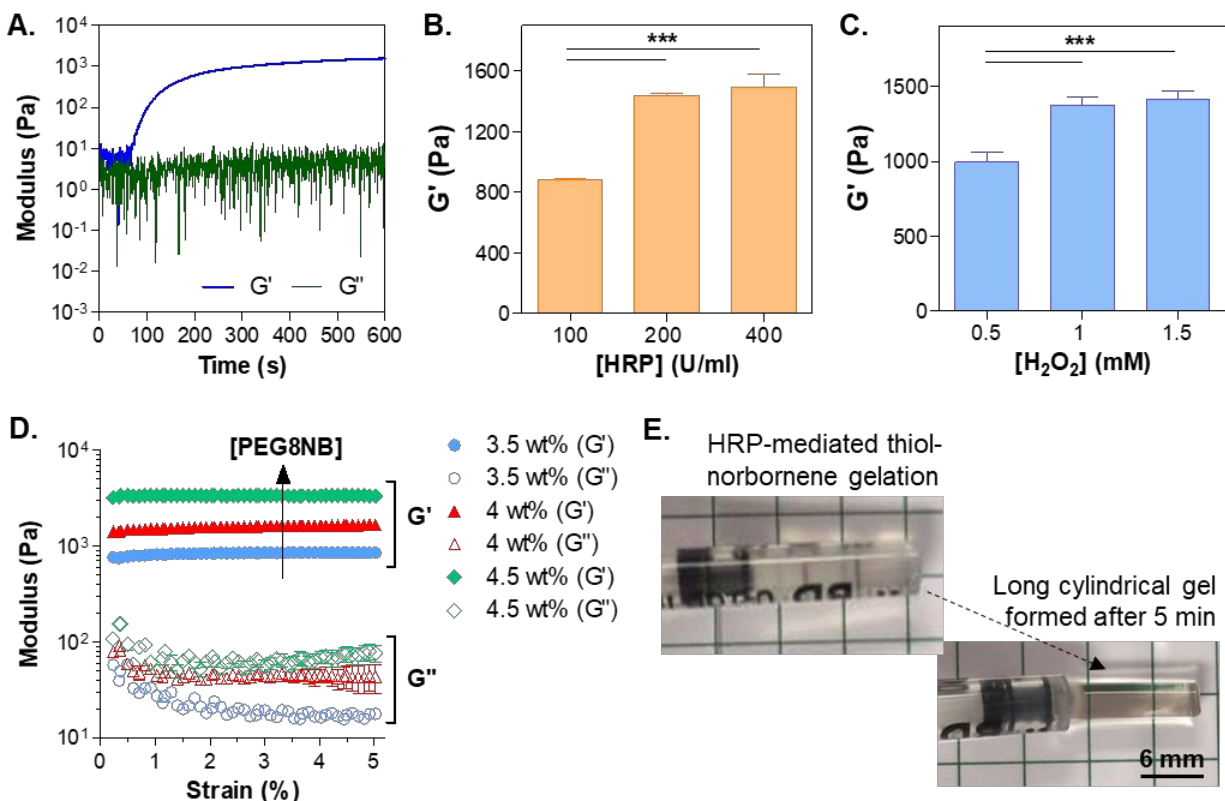
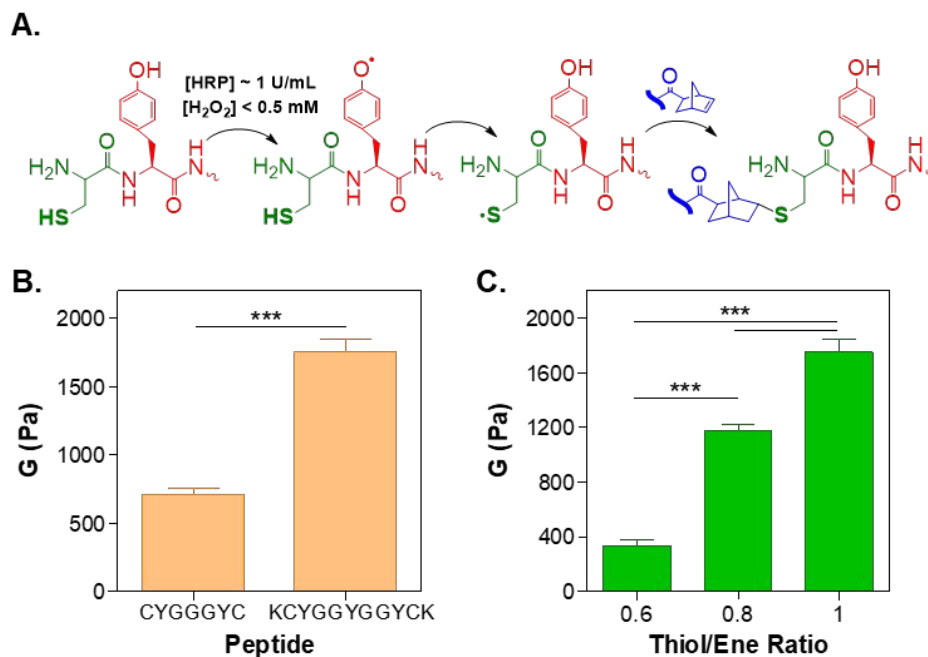


**Figure 2. Characterization of HRP-mediated thiol-norbornene hydrogelation.** (A) In situ rheometry of HRP-initiated thiol-norbornene gelation (all components: 3.5 wt% PEG8NB, 14 mM DTT, 200 U/ml HRP, 0.5 mM  $H_2O_2$ ). Effect of (B) HRP concentrations and (C)  $H_2O_2$  concentration on shear moduli of PEG8NB-DTT hydrogels. Gelation was formed with 3.5 wt% PEG8NB, and 14 mM DTT,  $R_{thiol/ene}=1$ .  $N = 3$ , mean  $\pm$  SEM. \*\*\* $p < 0.001$ ). (D) Strain-sweep rheometry of thiol-norbornene hydrogels formed with different macromer contents (Circles, triangles, and diamonds represent 3.5, 4, and 4.5 wt% PEG8NB, respectively.  $R_{thiol/ene} = 1$ ). (E) HRP-crosslinked thiol-norbornene hydrogel with a diameter of  $\sim 4$  mm and a length of  $\sim 15$  mm (200 U/mL HRP, 0.5 mM  $H_2O_2$ , 3.5 wt% PEG8NB, and 14 mM DTT).



26  
27  
28  
29  
30  
31  
32  
33  
34  
35  
36  
37  
38  
39  
40  
41  
42  
43  
44  
45  
46  
47  
48  
49  
50  
51  
52  
53  
54  
55  
56  
57  
58  
59  
60

**Figure 3. Effect of tyrosine residue on HRP-mediated crosslinking of thiol-norbornene PEG-peptide hydrogels.** (A) Proposed schematic of thiol radical generation via tyrosine residues. Effect of (B) tyrosine concentration and (C) thiol to norbornene ratio on the shear moduli of hydrogels ( $n=3$ , Mean  $\pm$  SEM, \*\*\* $p<0.001$ ).

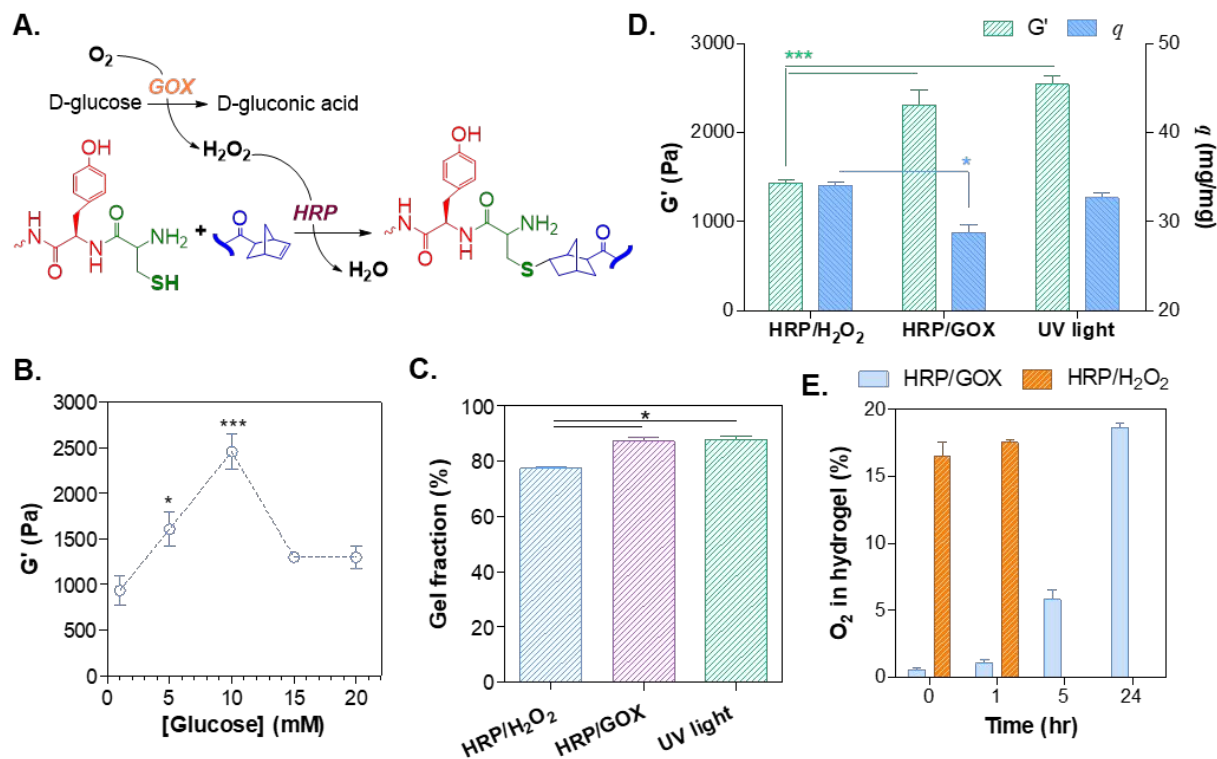


**Figure 4. Thiol-norbornene gelation initiated by tandem enzymatic reactions.** (A) Schematic of thiol-norbornene hydrogel formation via GOX and HRP-mediated crosslinking. (B) Effect of glucose concentration on shear moduli of dual enzyme-crosslinked thiol-norbornene hydrogels (1 U/mL HRP, 10 U/ml GOX, 3 wt% PEG8NB, and 12 mM CYGGGYC). (C) Gel fraction of hydrogels formed by HRP/H<sub>2</sub>O<sub>2</sub>, HRP/GOX, and UV light-mediated thiol-norbornene polymerization. Enzyme-crosslinked gels were prepared with 3.5 wt.% PEG8NB and 14mM DTT using HRP (200 U/mL), H<sub>2</sub>O<sub>2</sub> (1 mM), or with HRP (200 U/mL), GOX (10 U/ml), and glucose (10 mM). UV (365 nm) light-polymerized gels were formed with 1 mM LAP with light irradiation for 2 minutes. (D) Swelling ratio (q) and shear modulus (G') of the hydrogels as described in (C). (E) Oxygen contents within hydrogels formed by HRP/GOX (1 U/ml HRP, 1 U/mL GOX, 10 mM glucose) and HRP/H<sub>2</sub>O<sub>2</sub> (1 U/mL HRP, 0.5 mM H<sub>2</sub>O<sub>2</sub>). In the HRP/H<sub>2</sub>O<sub>2</sub> group, data were recorded only at 0 and 1-hr since O<sub>2</sub> levels were close to normoxia in both measurements (All experiments: n=3, Mean ± SEM, \*p<0.05 \*\*\*p<0.001).

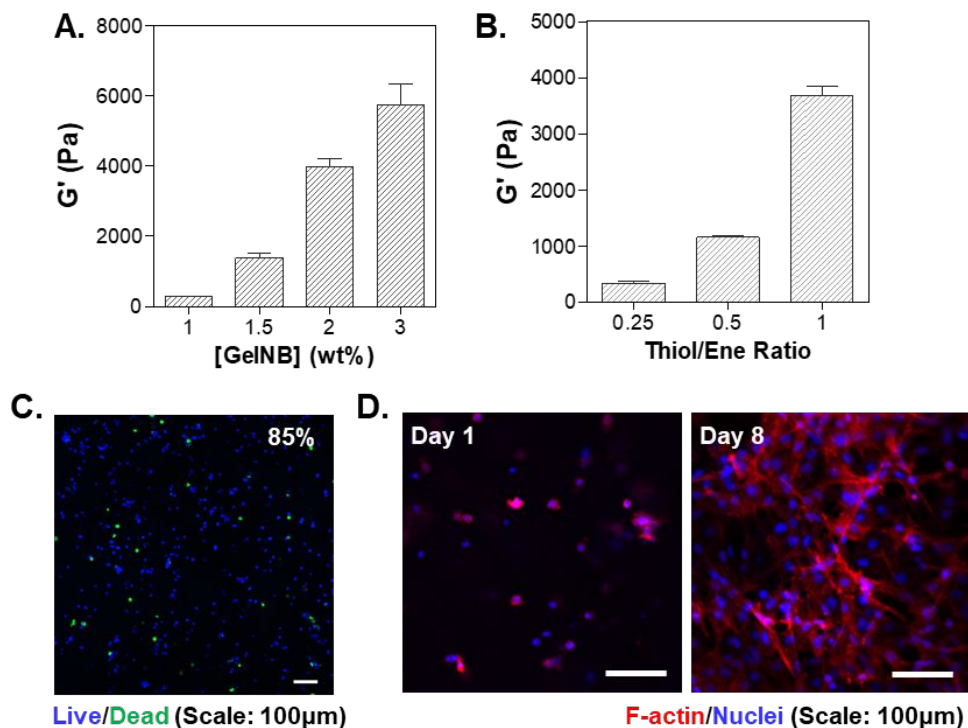


**Figure 5. Cytocompatibility of HRP-mediated GelNB-PEG4SH hydrogels.** Effect of gelatin content (A) and thiol-to-norbornene ratio (B) on shear moduli of GelNB-PEG4SH hydrogels (100 U/ml HRP, 10 U/ml GOX, 10 mM glucose.  $n \geq 3$ , Mean  $\pm$  SEM). (C) Live/Dead staining images of NIH/3T3 fibroblasts cultured in GelNB-PEG4SH hydrogels 24 hrs after encapsulation. (D) Fluorescence staining images of F-actin and nuclei in the encapsulated NIH/3T3 fibroblasts. Cell-laden gels were formed with 1.5 wt% GelNB-PEG4SH, 100 U/ml, and 0.5 mM  $\text{H}_2\text{O}_2$ .



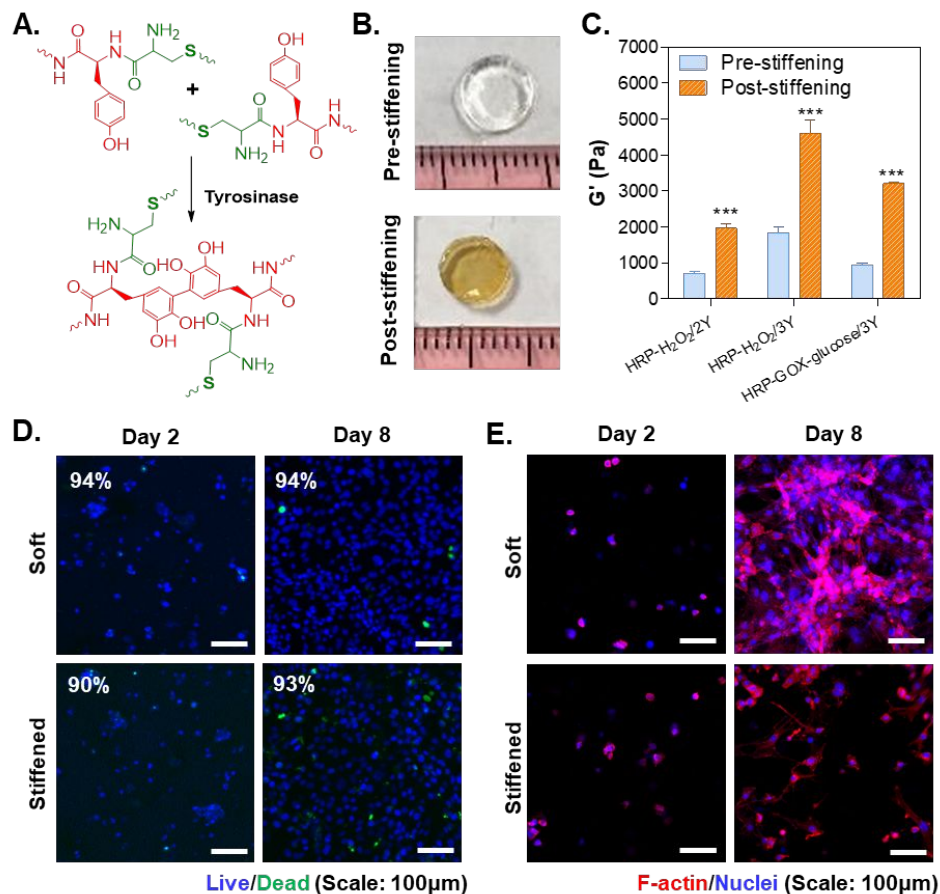


**Figure 6. Orthogonal enzymatic reactions for crosslinking and dynamic stiffening of PEG-peptide hydrogels.** (A) Schematic of MT-induced post-gelation dynamic crosslinking. (B) Photographs of enzymatically crosslinked PEG-peptide (2.5 wt% PEG8NB and KCYGGYGGYCK (3Y) thiol-norbornene hydrogels pre- and post-stiffening. Gel crosslinking was initiated by 1 U/mL HRP, 10 U/mL GOX, and 10mM glucose. Stiffening was induced by incubating the swollen gels in PBS containing 1 kU/mL MT. (C) Shear moduli of hydrogels pre- and post-stiffening. HRP = 1 u/ml, HRP/ $H_2O_2$  hydrogels were made with 3 wt% PEG8NB, while HRP/GOX-glucose were made with 2.5 wt% PEG8NB ( $n=3$ , Mean  $\pm$  SEM, \*\*\* $p<0.001$ ). (D) Live/dead staining images 48 hrs after encapsulation. Stiffened group were treated with 1 kU/ml MT for 6 hours on day 1. Hydrogels were made with 3 wt% PEG8NB-KCYGGYGGYCK (1 U/ml HRP, 0.5 mM  $H_2O_2$ ,  $G' \sim 1,500$  Pa). (E) F-actin and nuclei staining of NIH/3T3 fibroblasts encapsulated in soft or MT-stiffened gels.

## References

- [1] Kharkar PM, Kiick KL, Kloxin AM. Designing degradable hydrogels for orthogonal control of cell microenvironments. *Chem Soc Rev.* **2013**, *42*, 7335-72. 10.1039/c3cs60040h.
- [2] Liu S, Dicker KT, Jia X. Modular and orthogonal synthesis of hybrid polymers and networks. *Chem Commun.* **2015**, *51*, 5218-37. 10.1039/c4cc09568e.
- [3] Lin C-C. Recent advances in crosslinking chemistry of biomimetic poly(ethylene glycol) hydrogels. *RSC advances.* **2015**, *5*, 39844-398583. 10.1039/c5ra05734e.
- [4] Lin C-C, Ki CS, Shih H. Thiol-norbornene photoclick hydrogels for tissue engineering applications. *J Appl Polym Sci.* **2015**, *132*, 41563. 10.1002/app.41563.
- [5] Fairbanks BD, Schwartz MP, Halevi AE, Nuttelman CR, Bowman CN, Anseth KS. A versatile synthetic extracellular matrix mimic via thiol-norbornene photopolymerization. *Adv Mater.* **2009**, *21*, 5005-10. 10.1002/adma.200901808.
- [6] Neumann AJ, Quinn T, Bryant SJ. Nondestructive evaluation of a new hydrolytically degradable and photo-clickable PEG hydrogel for cartilage tissue engineering. *Macromol Biosci.* **2016**, *39*, 1-11. 10.1002/mabi.201700107.
- [7] Dadoo N, Landry SB, Bomar JD, Gramlich WM. Synthesis and Spatiotemporal Modification of Biocompatible and Stimuli-Responsive Carboxymethyl Cellulose Hydrogels Using Thiol-Norbornene Chemistry. *Macromol Biosci.* **2017**, *17*, 10.1002/mabi.201700107.
- [8] Pereira RF, Barrias CC, Bartolo PJ, Granja PL. Cell-instructive pectin hydrogels crosslinked via thiol-norbornene photo-click chemistry for skin tissue engineering. *Macromol Rapid Commun.* **2018**, *66*, 282-93. 10.1002/marc.201800181.
- [9] Van Hoorick J, Gruber P, Markovic M, Rollot M, Graulus GJ, Vagenende M, et al.; Highly Reactive Thiol-Norbornene Photo-Click Hydrogels: Toward Improved Processability. *Macromol Rapid Comm.* **2018**, 1800181. 10.1002/marc.201800181.
- [10] Shih H, Lin C-C. Cross-linking and degradation of step-growth hydrogels formed by thiol-ene photoclick chemistry. *Biomacromolecules.* **2012**, *13*, 2003-12. 10.1021/bm300752j.
- [11] Lin C-C, Raza A, Shih H. PEG hydrogels formed by thiol-ene photo-click chemistry and their effect on the formation and recovery of insulin-secreting cell spheroids. *Biomaterials.* **2011**, *32*, 9685-95. 10.1016/j.biomaterials.2011.08.083.
- [12] Gramlich WM, Kim IL, Burdick JA. Synthesis and orthogonal photopatterning of hyaluronic acid hydrogels with thiol-norbornene chemistry. *Biomaterials.* **2013**, *34*, 9803-11. 10.1016/j.biomaterials.2013.08.089.
- [13] Fraser AK, Ki CS, Lin C-C. PEG-based microgels formed by visible-light-mediated thiol-ene photo-click reactions. *Macromol Chem Phys.* **2014**, *215*, 507-15. 10.1002/macp.201300731.
- [14] Shin DS, Tokuda EY, Leight JL, Miksch CE, Brown TE, Anseth KS. Synthesis of Microgel Sensors for Spatial and Temporal Monitoring of Protease Activity. *ACS Biomater Sci Eng.* **2017**, *4*, 378-87. 10.1021/acsbomaterials.7b00017.
- [15] Shih H, Mirmira RG, Lin C-C. Visible light-initiated interfacial thiol-norbornene photopolymerization for forming an islet surface conformal coating. *J Mater Chem B.* **2015**, *3*, 170-5. 10.1039/c4tb01593b.

- 1  
2  
3 [16] Shih H, Lin C-C. Visible-light-mediated thiol-ene hydrogelation using eosin-Y as the only  
4 photoinitiator. *Macromol Rapid Comm.* **2013**, *34*, 269-73. 10.1002/marc.201200605.  
5  
6 [17] Batchelor R, Kwandou G, Spicer P, Stenzel M. (–)-Riboflavin (vitamin B2) and flavin  
7 mononucleotide as visible light photo initiators in the thiol–ene polymerisation of PEG-  
8 based hydrogels. *Polym Chem.* **2017**, *8*, 980-4. 10.1039/C6PY02034H.  
9  
10 [18] Jivan F, Fabela N, Davis Z, Alge DL. Orthogonal click reactions enable the synthesis of  
11 ECM-mimetic PEG hydrogels without multi-arm precursors. *J Mater Chem B.* **2018**, *6*,  
12 4929-36. 10.1039/C8TB01399C.  
13  
14 [19] Ooi HW, Mota C, ten Cate AT, Calore A, Moroni L, Baker MB. Thiol–Ene Alginate  
15 Hydrogels as Versatile Bioinks for Bioprinting. *Biomacromolecules.* **2018**, *19*, 3390-400.  
16 10.1021/acs.biomac.8b00696.  
17  
18 [20] McGann CL, Dumm RE, Jurusik AK, Sidhu I, Kiick KL. Thiol-ene Photocrosslinking of  
19 Cytocompatible Resilin-Like Polypeptide-PEG Hydrogels. *Macromol Biosci.* **2016**, *16*, 129-  
20 38. 10.1002/mabi.201500305.  
21  
22 [21] Elisseeff J, Anseth K, Sims D, McIntosh W, Randolph M, Langer R. Transdermal  
23 photopolymerization for minimally invasive implantation. *Proc Natl Acad Sci U S A.* **1999**,  
24 *96*, 3104-7. 10.1073/pnas.96.6.3104.  
25  
26 [22] Zavada S, McHardy N, Scott T. Oxygen-mediated enzymatic polymerization of thiol–ene  
27 hydrogels. *J Mater Chem B.* **2014**, *2*, 2598-605. 10.1039/C3TB21794A.  
28  
29 [23] Sakai S, Nakahata M. Horseradish Peroxidase Catalyzed Hydrogelation for Biomedical,  
30 Biopharmaceutical, and Biofabrication Applications. *Chem Asian J.* **2017**, *12*, 3098-109.  
31 10.1002/asia.201701364.  
32  
33 [24] Khanmohammadi M, Dastjerdi MB, Ai A, Ahmadi A, Godarzi A, Rahimi A, et al.;  
34 Horseradish peroxidase-catalyzed hydrogelation for biomedical applications. *Biomater Sci.*  
35 **2018**, *6*, 1286-98. 10.1039/c8bm00056e.  
36  
37 [25] Partlow BP, Hanna CW, Rnjak-Kovacina J, Moreau JE, Applegate MB, Burke KA, et al.;  
38 Highly tunable elastomeric silk biomaterials. *Adv Funct Mater.* **2014**, *24*, 4615-24.  
39 10.1002/adfm.201400526.  
40  
41 [26] Zhang Y, Tsitkov S, Hess H. Proximity does not contribute to activity enhancement in the  
42 glucose oxidase–horseradish peroxidase cascade. *Nat Commun.* **2016**, *7*, 13982.  
43 10.1038/ncomms13982.  
44  
45 [27] Kim BY, Lee Y, Son JY, Park KM, Park KD. Dual Enzyme-Triggered In Situ Crosslinkable  
46 Gelatin Hydrogels for Artificial Cellular Microenvironments. *Macromol Biosci.* **2016**, *16*,  
47 1570-6. 10.1002/mabi.201600312.  
48  
49 [28] Gantumur E, Sakai S, Nakahata M, Taya M. Cytocompatible enzymatic hydrogelation  
50 mediated by glucose and cysteine residues. *ACS Macro Lett.* **2017**, *6*, 485-8.  
51 10.1021/acsmacrolett.7b00122.  
52  
53 [29] Danielson AP, Bailey-Van Kuren D, Lucius ME, Makaroff K, Williams C, Page RC, et al.;  
54 Well-Defined Macromolecules Using Horseradish Peroxidase as a RAFT Initiase.  
55 *Macromol Rapid Commun.* **2016**, *37*, 362-7. 10.1002/marc.201500633.  
56  
57 [30] Carthew J, Frith J, Forsythe J, Truong V. Polyethylene glycol–gelatin hydrogels with  
58 tuneable stiffness prepared by horseradish peroxidase-activated tetrazine–norbornene  
59 ligation. *J Mater Chem B.* **2018**, *6*, 1394-401. 10.1039/C7TB02764H.  
60

- 1  
2  
3 [31] Fairbanks BD, Schwartz MP, Bowman CN, Anseth KS. Photoinitiated polymerization of  
4 PEG-diacrylate with lithium phenyl-2,4,6-trimethylbenzoylphosphinate: polymerization rate  
5 and cytocompatibility. *Biomaterials*. **2009**, *30*, 6702-7. 10.1016/j.biomaterials.2009.08.055.  
6
- 7 [32] Anderson SB, Lin C-C, Kuntzler DV, Anseth KS. The performance of human mesenchymal  
8 stem cells encapsulated in cell-degradable polymer-peptide hydrogels. *Biomaterials*. **2011**,  
9 *32*, 3564-74. 10.1016/j.biomaterials.2011.01.064.
- 10 [33] Liu HY, Nguyen HD, Lin CC. Dynamic PEG–Peptide Hydrogels via Visible Light and  
11 FMN-Induced Tyrosine Dimerization *Adv Healthcare Mater*. **2018**, *7*, 1870082.  
12 10.1002/adhm.201800954.  
13
- 14 [34] Lin T-Y, Ki CS, Lin C-C. Manipulating hepatocellular carcinoma cell fate in orthogonally  
15 cross-linked hydrogels. *Biomaterials*. **2014**, *35*, 6898-906.  
16 10.1016/j.biomaterials.2014.04.118.  
17
- 18 [35] Steward AJ, Kelly DJ. Mechanical regulation of mesenchymal stem cell differentiation. *J*  
19 *Anat*. **2015**, *227*, 717-31. 10.1111/joa.12243.
- 20 [36] Engler AJ, Sen S, Sweeney HL, Discher DE. Matrix elasticity directs stem cell lineage  
21 specification. *Cell*. **2006**, *126*, 677-89. 10.1016/j.cell.2006.06.044.  
22
- 23 [37] Huebsch N, Arany PR, Mao AS, Shvartsman D, Ali OA, Bencherif SA, et al.; Harnessing  
24 traction-mediated manipulation of the cell/matrix interface to control stem-cell fate. *Nat*  
25 *Mater*. **2010**, *9*, 518. 10.1038/nmat2732.  
26
- 27 [38] Levental KR, Yu H, Kass L, Lakins JN, Egeblad M, Ertler JT, et al.; Matrix crosslinking  
28 forces tumor progression by enhancing integrin signaling. *Cell*. **2009**, *139*, 891-906.  
29 10.1016/j.cell.2009.10.027.
- 30 [39] Liu HY, Greene T, Lin TY, Dawes CS, Korc M, Lin C-C. Enzyme-mediated stiffening  
31 hydrogels for probing activation of pancreatic stellate cells. *Acta Biomater*. **2017**, *48*, 258-  
32 69. 10.1016/j.actbio.2016.10.027.  
33
- 34 [40] Liu HY, Korc M, Lin C-C. Biomimetic and enzyme-responsive dynamic hydrogels for  
35 studying cell-matrix interactions in pancreatic ductal adenocarcinoma. *Biomaterials*. **2018**,  
36 *160*, 24-36. 10.1016/j.biomaterials.2018.01.012.  
37
- 38 [41] Acerbi I, Cassereau L, Dean I, Shi Q, Au A, Park C, et al.; Human breast cancer invasion  
39 and aggression correlates with ECM stiffening and immune cell infiltration. *Integr Biol*.  
40 **2015**, *7*, 1120-34. 10.1039/C5IB00040H.
- 41 [42] Caliarì SR, Perepelyuk M, Soulas EM, Lee GY, Wells RG, Burdick JA. Gradually softening  
42 hydrogels for modeling hepatic stellate cell behavior during fibrosis regression. *Integr Biol*.  
43 **2016**, *8*, 720-8. 10.1039/c6ib00027d.  
44
- 45 [43] Wang H, Haeger SM, Kloxin AM, Leinwand LA, Anseth KS. Redirecting valvular  
46 myofibroblasts into dormant fibroblasts through light-mediated reduction in substrate  
47 modulus. *PLoS One*. **2012**, *7*, e39969. 10.1371/journal.pone.0039969.  
48
- 49 [44] Moriyama K, Minamihata K, Wakabayashi R, Goto M, Kamiya N. Enzymatic preparation of  
50 a redox-responsive hydrogel for encapsulating and releasing living cells. *Chem Commun*.  
51 **2014**, *50*, 5895-8. 10.1039/c3cc49766f.
- 52 [45] Shih H, Liu HY, Lin C-C. Improving gelation efficiency and cytocompatibility of visible light  
53 polymerized thiol-norbornene hydrogels via addition of soluble tyrosine. *Biomater Sci*.  
54 **2017**, *5*, 589-99. 10.1039/c6bm00778c.  
55  
56  
57  
58  
59  
60

- 1  
2  
3 [46] Mishina M, Minamihata K, Moriyama K, Nagamune T. Peptide Tag-Induced Horseradish  
4 Peroxidase-Mediated Preparation of a Streptavidin-Immobilized Redox-Sensitive Hydrogel.  
5 *Biomacromolecules*. **2016**, *17*, 1978-84. 10.1021/acs.biomac.6b00149.  
6  
7 [47] Dawes CS, Konig H, Lin CC. Enzyme-immobilized hydrogels to create hypoxia for in vitro  
8 cancer cell culture. *Journal of biotechnology*. **2017**, *248*, 25-34.  
9 10.1016/j.jbiotec.2017.03.007.  
10  
11 [48] Kleppe K. The effect of hydrogen peroxide on glucose oxidase from *Aspergillus niger*.  
12 *Biochemistry*. **1966**, *5*, 139-43. 10.1021/bi00865a018.  
13  
14 [49] Blandino A, Macías M, Cantero D. Modelling and simulation of a bienzymatic reaction  
15 system co-immobilised within hydrogel-membrane liquid-core capsules. *Enzyme Microb*  
16 *Technol*. **2002**, *31*, 556-65. 10.1016/S0141-0229(02)00154-0.  
17  
18 [50] Tse PH, Gough DA. Time-dependent inactivation of immobilized glucose oxidase and  
19 catalase. *Biotechnol Bioeng*. **1987**, *29*, 705-13. 10.1002/bit.260290607.  
20  
21 [51] Baynton KJ, Bewtra JK, Biswas N, Taylor KE. Inactivation of horseradish peroxidase by  
22 phenol and hydrogen peroxide: a kinetic investigation. *Biochim Biophys Acta*. **1994**, *1206*,  
272-8. 10.1016/0167-4838(94)90218-6.  
23  
24 [52] Park KM, Gerecht S. Hypoxia-inducible hydrogels. *Nat commun*. **2014**, *5*, 4075.  
25 10.1038/ncomms5075.  
26  
27 [53] Hung SP, Ho JH, Shih YRV, Lo T, Lee OK. Hypoxia promotes proliferation and osteogenic  
28 differentiation potentials of human mesenchymal stem cells. *J Orthop Res*. **2012**, *30*, 260-6.  
29 10.1002/jor.21517.  
30  
31 [54] Munoz Z, Shih H, Lin C-C. Gelatin hydrogels formed by orthogonal thiol-norbornene  
32 photochemistry for cell encapsulation. *Biomater Sci*. **2014**, *2*, 1063-72.  
33 10.1039/c4bm00070f.  
34  
35 [55] Greene T, Lin C-C. Modular cross-linking of gelatin-based thiol-norbornene hydrogels for in  
36 vitro 3D culture of hepatocellular carcinoma cells. *ACS Biomater Sci Eng*. **2015**, *1*, 1314-  
37 23. 10.1021/acsbiomaterials.5b00436.  
38  
39 [56] Shih H, Greene T, Korc M, Lin C-C. Modular and Adaptable Tumor Niche Prepared from  
40 Visible Light Initiated Thiol-Norbornene Photopolymerization. *Biomacromolecules*. **2016**,  
41 *17*, 3872-82. 10.1021/acs.biomac.6b00931.  
42  
43 [57] Greene T, Lin TY, Andrisani OM, Lin CC. Comparative study of visible light polymerized  
44 gelatin hydrogels for 3D culture of hepatic progenitor cells. *J Appl Polym Sci*. **2017**, *134*,  
45 10.1002/app.44585  
46  
47 [58] Park KM, Shin YM, Joung YK, Shin H, Park KD. In situ forming hydrogels based on  
48 tyramine conjugated 4-Arm-PPO-PEO via enzymatic oxidative reaction.  
49 *Biomacromolecules*. **2010**, *11*, 706-12. 10.1021/bm9012875.  
50  
51 [59] Guvendiren M, Burdick JA. Stiffening hydrogels to probe short- and long-term cellular  
52 responses to dynamic mechanics. *Nat Commun*. **2012**, *3*, 792. 10.1038/ncomms1792.  
53  
54 [60] Caliarì SR, Perepelyuk M, Cosgrove BD, Tsai SJ, Lee GY, Mauck RL, et al.; Stiffening  
55 hydrogels for investigating the dynamics of hepatic stellate cell mechanotransduction  
56 during myofibroblast activation. *Sci Rep*. **2016**, *6*, 21387. 10.1038/srep21387.  
57  
58 [61] Rosales AM, Vega SL, DelRio FW, Burdick JA, Anseth KS. Hydrogels with Reversible  
59 Mechanics to Probe Dynamic Cell Microenvironments. *Angew Chem Int Ed*. **2017**, *56*,  
60 12132-6. 10.1002/anie.201705684.

- 1  
2  
3 [62] Payen T, Palermo CF, Sastra SA, Chen H, Han Y, Olive KP, et al.; Elasticity mapping of  
4 murine abdominal organs in vivo using harmonic motion imaging (HMI). *Phys Med Biol.*  
5 **2016**, *61*, 5741-54. 10.1088/0031-9155/61/15/5741.  
6  
7 [63] Bainbridge P. Wound healing and the role of fibroblasts. *J Wound Care.* **2013**, *22*,  
8 10.12968/jowc.2013.22.8.407.  
9  
10 [64] Raza A, Lin C-C. The Influence of Matrix Degradation and Functionality on Cell Survival  
11 and Morphogenesis in PEG-Based Hydrogels. *Macromol Biosci.* **2013**, *13*, 1048-58.  
12 10.1002/mabi.201300044.  
13  
14  
15  
16  
17  
18  
19  
20  
21  
22  
23  
24  
25  
26  
27  
28  
29  
30  
31  
32  
33  
34  
35  
36  
37  
38  
39  
40  
41  
42  
43  
44  
45  
46  
47  
48  
49  
50  
51  
52  
53  
54  
55  
56  
57  
58  
59  
60

1  
2  
3 **For Table of Contents Use Only**  
4

5  
6 ***Enzymatic crosslinking of dynamic thiol-norbornene click hydrogels***  
7

8 Han D. Nguyen, Hung-Yi Liu, Britney N. Hudson, and Chien-Chi Lin  
9

10 *Department of Biomedical Engineering, Purdue School of Engineering & Technology,*  
11 *Indiana University-Purdue University Indianapolis, Indianapolis, IN 46202, USA*  
12  
13  
14

